Supporting Information

"Bubbles-Linking-Bubble" Hybrid Fibers Filled with Ultrafine TiN: A

Robust and Efficient Platform Achieving Fast Kinetics, Strong Ion

Anchor and High Areal Loading for Selenium Sulfide

Bing Han[a, †], Xiaolong Li[a,†], Yang Zhou[a, b], Xiaohui Gao[c], Weili Qu[a,c,*], Sen Zhang[b,*]

and Chao Deng[a,*]

[a]Key Laboratory for Photonic and Electronic Bandgap Materials, Ministry of Education;

Key Laboratory of Photochemical Biomaterials and Energy Storage Materials,

Heilongjiang Province; Harbin Normal University, Harbin, 150025, Heilongjiang, China.

[b]Key Laboratory of Superlight Material and Surface Technology, Ministry of Education;

College of Material Science and Chemical Engineering, Harbin Engineering University,

150025, Heilongjiang, China.

[c]Northeast Agriculture University, 150025, Heilongjiang, China.

Corresponding Author

E-Mail: chaodenghsd@sina.com (C. Deng);

senzhang@hrbeu.edu.cn (S. Zhang)

Part I: Experimental details, Calculations & Discussions

S-1-1: Preparation of the BLB hybrid fiber

i) Preparation of the precursor by dual-nozzle electrospinning

Firstly, the dual-nozzle with the coaxial structure was used in the electrospinning to prepare the precursor. On the one hand, the shell solution was prepared by dissolving the polyvinyl pyrrolidone (PVP, MW:1300000, Aladdin, Shanghai, China) in the absolute ethanol (Aladdin, Shanghai, China) at room temperature under continuous stirring. On the other hand, the tetrabutyl titanate (TBOT, Aladdin, shanghai, China) was mixed with acetic acid (Aladdin, shanghai, China) at room temperature, and then the mixture was mixed with the silicone oil (Aladdin, shanghai, China) to form the core solution. The dual-nozzle was constructed by two coaxial needles, *i.e.* the 23-gauge inner needle (OD: 0.63 mm, ID: 0.33 mm) and the 17-gauge outer needle (OD: 1.47 mm, ID: 1.07 mm). The core solution was loaded into the syringe connected to the inner channel of a dual nozzle and the shell solution was loaded into the syringe connected to the outer channel. A high voltage of 10~12 kV was applied on the dual nozzle and the distance between the needle and the rotating drum collector was ~9 cm. The feeding rate of the shell solution was kept at 1.5 ml h^{-1} and that of the core solution was adjusted to control the structure of the hybrid fiber. After the electrospinning process, the film was peeled off from the collector and the precursor was achieved.

ii) Preparation of the BLB hybrid fiber

The electrospinning precursor was initially stabilized at 280 ^{o}C in air. Then the product was calcinated at 700 ^{o}C in N$_2$ atmosphere and followed by in NH$_3$ atmosphere. After

etching out the residual silicate oxide impurities by HF solution, the BLB hybrid fiber was achieved.

S-1-2: Synthesis of reference host samples

In addition, two samples prepared by modified conditions were employed as reference samples.

i) For the preparation of the CF reference sample, the core solution for the inner channel was only the mixture of acetic acid and silicone oil. The other synthetic conditions, including the shell solution, the electrospinning process and the calcination process were all the same as the BLB hybrid fiber.

ii) For the preparation of the HB reference sample, the core solution for the inner channel was only the silicone oil. The other synthetic conditions, including the shell solution, the electrospinning process and the calcination process were all the same as the BLB hybrid fiber.

S-1-3: Preparation of the freestanding selenium sulfide electrode

The melting diffusion method was employed to prepare the freestanding selenium sulfide electrodes. The SeS_2 powder was firstly dissolved into the toluene, which was then dripped onto the film of BLB hybrid fiber. The weight ratio of carbon host to selenium sulfide is about 3: 8.

Then film was put into a closed glass container and calcinated at 180 ^{o}C to enable the selenium sulfide infiltrate into the pores of the hosts. After cooling to the room temperature, the selenium sulfide@BLB hybrid fiber freestanding electrode was obtained. The same procedure was used to build the electrode based on the CF and HB hosts.

S-2: Materials characterizations

Powder X-ray diffraction (XRD, Bruker D8/Germany) using Cu Kα radiation was employed to identify the crystalline phase of the material. The experiment was performed by using step mode with a fixed time of 3 *s* and a step size of 0.02^o. The XRD pattern was refined by using the Rietveld method. The morphology was observed with a scanning electron microscope (SEM, HITACHIS-4700) and a transmission electron microscope (TEM, JEOS-2010 PHILIPS). The element distribution of the sample was confirmed by energy dispersive X-ray detector (EDX). Thermogravimetric analysis (TGA, NETZSCH STA 449C) was used to monitor the decomposition process of the precursor and its components. Nitrogen adsorption-desorption isotherms were measured using a Micromeritics ASAP 2010. Sample preparation included degassing at 378 K (105 ^{o}C) for 10 h in a vacuum of 10^{-6} Torr. The treating temperature for the BET testing has been carefully discussed in Figure S7. Specific surface area and pore size distribution were calculated using the Brunauer-Emmett-Teller (BET) and Barrett-Joyner-Halenda (BJH) method, respectively.

S-3: Electrochemical measurements

The electrochemical characteristics were measured in coin cells. The prepared freestanding electrodes were directly used as the working electrode without additional components such as binder, conductive additive or current collector. The coin cells were assembled in an argon filled glove box. The lithium foil was employed as counter and reference electrode and the Celgard 2300 microporous polypropylene membrane was used as separator. The electrolyte was composed of 1 mol·L^{-1} lithium bis(trifluoromethanesulfonyl)imide (LiTFSI) and 0.2 mol·L^{-1} LiNO$_3$ in 1,3-dioxolane

(DOL) and 1,2-dimethoxyethane (DME) (v:v=1:1). Galvanostatic charge/discharge tests were performed in the potential range of 1.8~2.8 V vs. Li$^+$/Li on a Land battery testing system (Wuhan, China).

S-4: Calculation methods

S-4-1: Calculation of the electrochemical parameters

(1) specific capacity (Q)

The specific capacity is calculated based on the galvanostatic charge/discharge curves,

$$Q = \frac{I \times \Delta t}{m} \qquad (1)$$

Where Q is the specific capacity, Δt is the discharge time, I is the discharge current, m is the mass of the active material in the single electrode.

(2) Cycling retention

The cycling retention is calculated based on the following equation,

$$CR = \frac{Q(after)}{Q(before)} \qquad (2)$$

Where CR is the capacitance retentions after cycling, Q (after) is the capacity of the electrode after cycling, Q (before) is the capacity of the electrode before cycling,
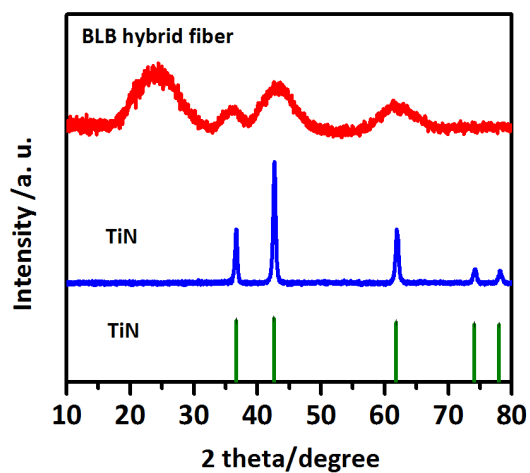
Part II: Supporting Figures

Figure S1

Figure S1 XRD patterns of the pristine TiN and the BLB hybrid fiber with filling TiN nanoparticles. The standard pattern for the TiN crystal is also displayed.

The pristine TiN nanoparticles were prepared by treating the core solution for the dual-nozzle electrospinning. The TBOT and acetic acid was mixed and then the mixture was dried in an oven at 80 ^{o}C overnight. Then the dried gel was calcinated at 700 ^{o}C in N_2 atmosphere and followed by in NH_3 atmosphere.
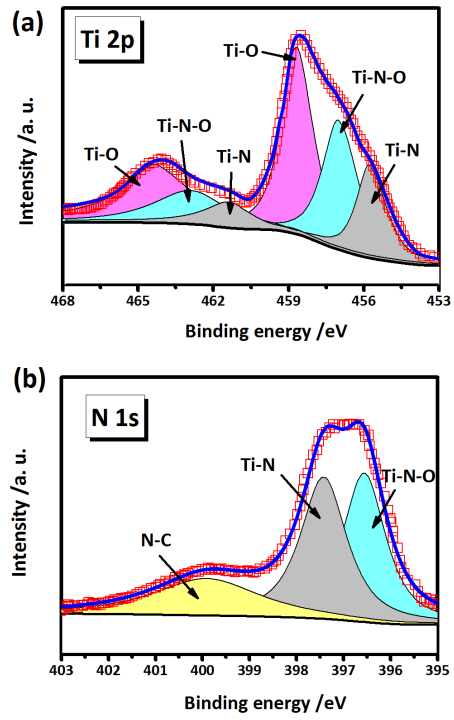
Figure S2

Figure S2 (a) Ti 2p and (b) N 1s XPS spectra of the TiN in the BLB hybrid fiber.
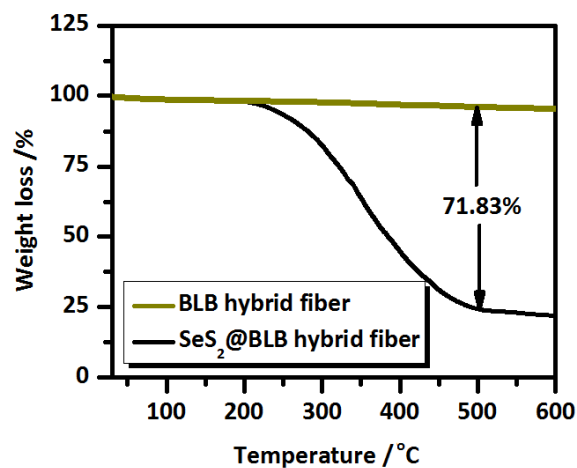
Figure S3

Figure S3 TG curves of the BLB hybrid fiber and the SeS$_2$@BLB hybrid fiber at a heating rate of 10 $^{\circ}$C min^{-1} in the N$_2$ atmosphere. The results show that the weight of the BLB hybrid fiber is stable till 600 $^{\circ}$C. After loading the selenium sulfide, the obvious weight loss of the electrode can be attributed to the loss of active material. Based on the results, the content of the SeS$_2$ in the freestanding electrode is about 71.83 wt.%.
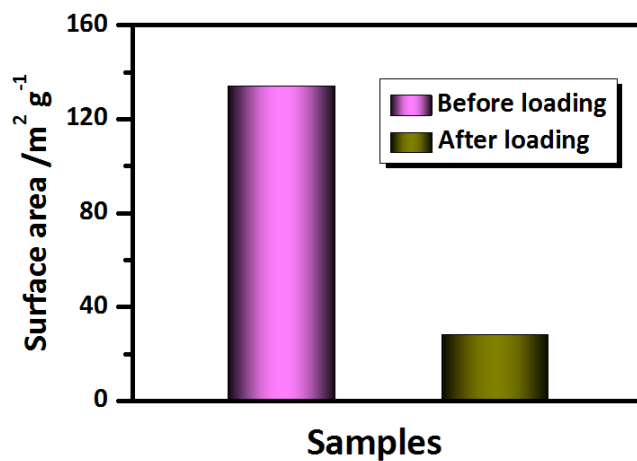
Figure S4

Figure S4 Comparison of the surface area of the BLB hybrid fiber before and after active material loading. The results show that the surface area of the BLB hybrid fiber obviously decreased after active material loading. However, the residual high surface areas after active material loading demonstrate the existence of the residual voids in the SeS_2@hybrid fiber.
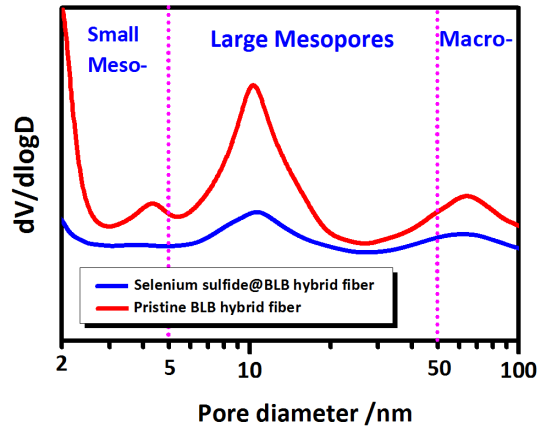
Figure S5

Figure S5 Pore size distribution curves of the selenium sulfide@BLB hybrid fiber and the pristine BLB hybrid fiber.
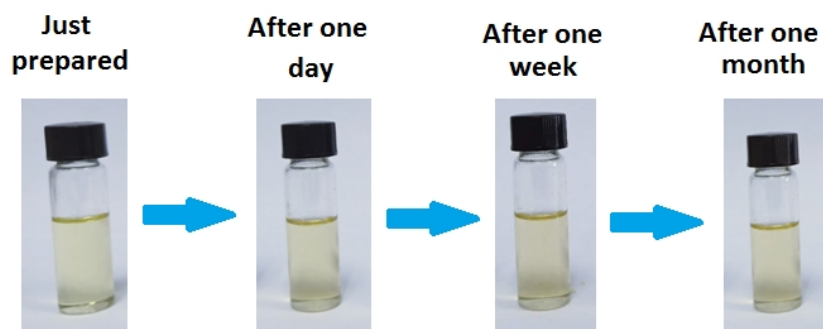
Figure S6

Figure S6 Digital photos of the mixed solution of TBOT and acetic acid. The uniform solution can keep for one month without appearance of any precipitates. The results demonstrate the high stability of the mixed sol in the core solution.
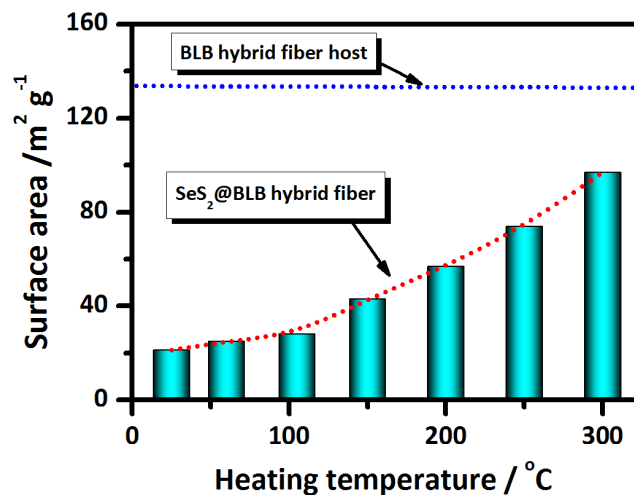
Figure S7

Figure S7 Comparison of the surface areas of the SeS_2@BLB hybrid fibers after different heating temperature before BET testing. The surface area of the pristine BLB hybrid fiber host is denoted by blue dot lines.

To clarify the effects of the heating temperature on the BET results, we used a series of heating temperatures of 25 °C, 70 °C, 105 °C, 150 °C, 200 °C, 250°C and 300 °C to treat the samples before BET testing. The heating time for all the temperatures is kept at 10 hours in a vacuum of 10^{-6} Torr. As displayed in Figure S7, as the temperature increases, the surface areas of the samples initially show no obvious change from room temperature to 105 °C. Then the surface areas of the samples quickly increase as the temperature further increases. Especially, when the heating temperature reaches 300 °C, the surface area of the SeS_2 loaded sample is near to that of the pristine carbon host. The results indicate that the treating temperature greatly affects the BET results of selenium

sulfide@BLB hybrid fiber. It is associated with the poor thermal stability of the selenium sulfide.

According to above thermal analysis result (Figure S3), the weight of the selenium sulfide@BLB hybrid fiber begins to decrease from 150 ^{o}C. As it increases to 200 ^{o}C, the obvious weight loss indicates that the poor stability of selenium sulfide at high temperature. As the temperature further increases, the dramatically weight loss of the sample indicates the quick lose of the active material. Therefore, the thermal analysis results demonstrate that the selenium sulfide will be lost from the BLB carbon host during high temperature treating before BET testing. The loss of active material in the selenium sulfide@BLB hybrid fiber will set free the surfaces of the pores. As a result, the higher surface area is achieved for samples under higher treating temperature.

Combined above results, the poor thermal stability of the selenium sulfide leads to the larger measured values of the surface areas for the selenium sulfide@BLB hybrid fiber. Therefore, the heating temperature should be controlled to be lower than 150 ^{o}C to decrease the measured error. In our experiment, the heating temperature of 105 ^{o}C is used to pretreat the samples before BET testing. It is considered as the optimal point that can well retain the active material and remove the absorbed water simultaneously.